Spring 2013

Characterization of calcium binding protein 1 (CaBP1/CD) expression and localization in the mouse brain

Kristin Kim
University of Iowa

CHARACTERIZATION OF CALCIUM BINDING PROTEIN 1 (CABP1/CD) EXPRESSION AND LOCALIZATION IN THE MOUSE BRAIN

by

Kristin Kim

A thesis submitted in partial fulfillment
of the requirements for the Master of
Science degree in Molecular Physiology and Biophysics
in the Graduate College of
The University of Iowa

May 2013

Thesis Supervisor: Associate Professor Amy Lee

Graduate College
The University of Iowa
Iowa City, Iowa

CERTIFICATE OF APPROVAL

_____

MASTER'S THESIS

_____

This is to certify that the Master's thesis of

Kristin Kim

has been approved by the Examining Committee
for the thesis requirement for the Master of Science
degree in Molecular Physiology and Biophysics
at the May 2013 graduation.

Thesis Committee: _____
Amy Lee, Thesis Supervisor

_____
N. Charles Harata

_____
C. Andrew Frank

To Mom, Joe and the birds.

ACKNOWLEDGMENTS

This work was supported by NIH grants EY020850, DC009433, HL087120, and a Carver Research Program of Excellence Award, University of Iowa Carver College of Medicine. I'd also like to thank Dr. D. P. Mohapatra and Dr. Andrew J. Shepherd for assistance and advice on immunohistochemical techniques.

ABSTRACT

Ca^{2+}-binding proteins (CaBP) alter Ca^{2+} signals, triggering cellular processes such as gene transcription regulation in neurons. CaBP1/CD is a calmodulin (CaM)-like Ca^{2+} binding protein that may regulate neuronal functions through interactions with effectors such as voltage-gated Ca^{2+} (Ca_v) channels and inositol trisphosphate receptors ($InsP_3Rs$). To gain insight into the potential cellular functions of CaBP1/CD, we analyzed the expression and localization of CaBP1/CD variants in mouse brain. Of the three CaBP1/CD splice variants that have been characterized (CaBP1-S, CaBP1-L, and caldendrin (CD)), CD was the major variant expressed in mouse brain by western blot and quantitative polymerase chain reaction. These results reflected the expression of CaBP1/CD since they were not reproduced in mice with targeted disruption of the gene encoding CaBP1/CD (CaBP1 knock-out). By immunoperoxidase labeling, CaBP1/CD was localized in multiple cell-types including pyramidal cells in the cerebral cortex and hippocampal CA3 neurons and inhibitory neurons in the cerebellum. In the cerebellum, CaBP1/CD was not detected in Purkinje neurons but strongly colocalized with voltage-sensitive *Shaker*-type potassium channel, $K_v1.2$, in the pinceau formation formed between basket cells and the Purkinje cell axon initial segment. We conclude that CaBP1/CD is expressed in a subset of principal neurons where it may regulate Ca^{2+} signaling and neuronal excitability.

TABLE OF CONTENTS

LIST OF TABLES

Table

LIST OF FIGURES

Figure

CHAPTER I.

INTRODUCTION

Calcium (Ca^{2+})-binding proteins regulate Ca^{2+} signaling by either binding to or modulating target proteins (Ca^{2+} sensors), or acting as buffers (Ca^{2+} buffers). Among the Ca^{2+}-binding protein superfamily members containing EF-hand Ca^{2+} binding domains, calmodulin (CaM) is highly conserved in eukaryotes and ubiquitously expressed in all cells. CaM contains two pairs of EF-hand motifs connected by a flexible central linker (Babu et al., 1985; Cheung, 1980; Crivici and Ikura, 1995; Haeseleer et al., 2002; Ikura et al., 1992; Yap et al., 1999). Upon binding to Ca^{2+} ions, CaM undergoes a conformational change, exposing its hydrophobic binding sites (Haeseleer et al., 2002; Meyer et al., 1996). CaM interacts with and regulates numerous kinases, ion channels, and other effectors, triggering many essential cellular events.

Ca^{2+}-Binding Protein 1 (CaBP1/CD) belongs to a family of EF-hand Ca^{2+} binding proteins that is abundantly expressed in the brain and retina (Haeseleer et al., 2000), but the physiological role of CaBP1/CD remains unclear. Similar to CaM, CaBP1/CD has four EF-hand motifs (EF-hand 1-4), but only three are functional (EF-hand 1, 3-4). Ca^{2+} cannot bind to EF-hand 2, which further inhibits cooperative Ca^{2+} binding to EF-hand 1 (Wingard et al., 2005). Compared to CaM, the central linker domain in CaBP1/CD is extended by one α-helical turn, which may significantly affect CaBP1/CD interactions with effectors (Haeseleer et al., 2000).

Three splice variants of CaBP1/CD exist that vary in length and their N-terminal regions (Haeseleer et al., 2000; Laube et al., 2002). Sequence alignments (Fig. 2A) revealed unique properties of these isoforms. CaBP1-S (short), CaBP1-L (long) and caldendrin (CD) share identical EF-hand organization while their N-terminal regions differ in length and structure. CaBP1-S and CaBP1-L contain an N-myristoylation site, which may be critical for its distinct

localization in transfected CHO cells (Haeseleer et al., 2000), whereas CD lacks this feature (Mikhaylova et al., 2006).

CaM and CaBP1/CD bind to the same target proteins like voltage-gated Ca^{2+} (Ca_v) channels, but CaBP1/ CD often has distinct modulatory properties compared to CaM (Haeseleer et al., 2004; Lee et al., 2002; Tippens and Lee, 2007; Yang et al., 2002; Zhou et al., 2004; Zhou et al., 2005). While CaM increases Ca^{2+}-dependent inactivation (CDI) of L-type Ca^{2+} (Ca_v1) channels, CaBP1/CD inhibits CDI (Tippens and Lee, 2007; Yang et al., 2006; Zhou et al., 2004). These results suggest that CaBP1 and CD may differentially modulate Ca^{2+} signals in neurons by competing with CaM for binding partners like Ca_v1 channels. Moreover, CaBP1/CD may interact with and modulate a specific group of targets different from that of CaM such as the transient receptor potential canonical type 5 (TRPC5) (Kinoshita-Kawada et al., 2005) further diversifying Ca^{2+} signaling.

To broaden our understanding of CaBP1 and CD role in the central nervous system, we analyzed the expression and localization of CaBP1/CD in mouse forebrain and cerebellum, and generated a CaBP1 knockout (KO) mouse. Consistent with previous findings, we observed CaBP1/CD labeling using CaBP1/CD antibodies in neurons throughout the brain, including in a subset of neurons in the hippocampus and cerebral cortex. Expanding from previous reports, we performed double immunofluorescence labeling and discovered localization of CaBP1/CD variants in presynaptic and postsynaptic compartments of GABA-ergic inhibitory interneurons.

We also analyzed the expression of CaBP1 splice variants by quantitative PCR, and demonstrate CD as the major CaBP1/CD variant expressed in the mouse brain. Additionally, we show that the two variants of CD detected in the brain (33-/36-kDa), may result from alternative translation start sites. We conclude that CaBP1/ CD localizes in a subpopulation of excitatory and

inhibitory neurons, where CD potentially modulates Ca^{2+}-dependent processes important for neuronal physiology.

CHAPTER II.

MATERIALS AND METHODS

Animals

Animal handling was approved by the University of Iowa Institutional Animal Care and Use Committee, and used in accordance with the National Institutes of Health guidelines. Forty-six genetically modified adult mice (2-5 months old, F2 generation) from a 129/SvEv and C57Bl6 mixed strain were used for immunohistochemistry, molecular biology, and biochemical analysis.

Construction of CaBP1/CD Targeting Vector

In order to generate a CaBP1/CD-deficient mouse, a targeting vector was constructed. An insertion of a 2.4 kilobase (kb) upstream of exon 1a, and a 5.8 kb fragment found downstream of exon 1b were amplified by PCR. The 2.4 kb insert was ligated into the targeting vector before an mCherry start site using NotI/NheI, and the 5.8 kb fragment was added downstream of a neomycin sequence (SalI). The final CaBP1/CD targeting construct was sent to the University of Iowa Gene Transfer Core Facility.

Generation of CaBP1/CD-deficient Mice

Embryonic stem cells (ES) from 129/SvEv strain were electroporated with the CaBP1/CD targeting vector at the University of Iowa Gene Transfer Core. Seven positive recombinant ES cells that were neomycin-resistant and expressed an mCherry sequence, assessed by polymerase chain reaction (PCR) (oAL676 forward 5'-GTGTGCAAGATAACCAGCTTC-'3; oAL655 reverse 5'-CATGGTCTTCTTCTGCATTAC-3'), were injected into host C57/Bl6 mouse blastocysts at the University of Iowa Gene Transfer Core Facility. Once chimeras were generated, they were crossed with C57/Bl6 mice in order to transmit the CaBP1/CD mutant gene into germ-line. Genomic DNA was extracted from pups, and the presence of the mutant allele was confirmed by genotyping.

Littermates carrying the mutant allele were mated to produce CaBP1 KO mice. The CaBP1 knockout was further validated by RT-PCR, immunoblotting and immunohistochemistry.

Genotyping

Genomic DNA was isolated from fresh mouse tissue. Fragments of the wild-type (WT) and knockout (KO) alleles were amplified by PCR using GoTaq Green Master Mix (Promega, Madison, WI) and 300 nanograms (ng) of genomic DNA. The following oligos primers were used in the PCR reaction: (oAL795 WT for. 5'-CTCGTGCTCACATTCAGTGC-3'; oAL796 WT rev. 5'-CAATGTGCGAGCTCATCG-3'; oAL797 KO rev. 5'-GATGATGGCCATGTTATCCTC-3'). PCR products were viewed under an ultraviolet transilluminator.

Reverse Transcriptase-Polymerase Chain Reaction (RT-PCR)

Total RNA was extracted from mouse brain tissue using TRIzol reagent (Life Technologies, Grand Island, NY). Brain cDNAs were synthesized using oligo (dT) primers from the Two-step Superscript III Kit (Life Technologies). By PCR methods, the expression of each variant was detected using isoform-specific primers (GAPDH for. 5'-CCTCTGGAAAGCTGTGGCGTGATGG-3'; rev. 5'-AGATCCACGACGGACACATT-3'; oAL701 CaBP1-S and –L for. 5'-CAAGTCGCCACTAAGAAACC-3'; oAL702 CD rev. 5'-CGGACCCGTTCCTCCAC-3'; oAL703 CaBP1/CD rev. 5'-GTTGATCTGCTGAGACAGCTC-3').

Quantitative RT-PCR (qRT-PCR)

Cortex, cerebellum, and hippocampus were dissected from 3-4 one-month-old mice. Total RNA was isolated using TRIzol Reagent (Life Technologies), and reverse transcription was performed with the SuperScript III First-Strand Synthesis System (Life Technologies). qRT-PCR was performed using the StepOnePlus Real-Time PCR system with TaqMan Gene Expression

assays for CaBP1 (accession number Mm01203518_m1) and CD. Life Technologies custom design tool was used to create an assay for CD, which recognizes CD coding regions from exon 1a to 2A (Fig. 1A). GAPDH was used as an endogenous normalizer. These assays were tested against CaBP1 and CD plasmid DNAs to verify the specificity of the assay for the intended target. Assays were also tested on serial dilutions of cDNA prepared from total brain RNA to verify that CD, CaBP1, and GAPDH assays demonstrated similar amplification efficiencies. ΔC_T values obtained from cortex, cerebellum, and hippocampus samples were averaged over three separate PCR experiments, with three technical replicates from each sample per experiment. The relative quantities (RQ) of CD and CaBP1 were calculated by the $\Delta\Delta C_T$ method using StepOne data analysis software. Error bar ranges represent the minimum (RQmin) and maximum (RQmax) possible RQ values calculated from a 95% confidence interval of C_T values.

CD Short and Long (CD-S AND -L) Isolation

Designed to isolate CD-S and CD-L fragments in WT mouse brain, CD-specific primers amplified each fragment using the following primers: oAL798 CD-S forward 5'-ATGAGCTCGCACATTGCC AAG-3'; oAL799 CD-L forward 5'- AGA GGCTGCGCTGTCACATG -3'; oAL800 common reverse 5'-TCAGCGAGACATCATCCGGAC-3'. PCR products were then ligated into pCR2.1TOPO vector (Life Technologies), excised, and inserted into CMV-promoter containing vector, pcDNA3.1+ (Life Technologies) using restriction sites EcoRI for CD-L and BamHI/XhoI for CD-S. The CD-S and -L constructs underwent sequencing analysis provided by the University of Iowa's DNA Sequencing Facility.

Antibodies

Polyclonal anti-CaBP1/CD rabbit antibodies (Haeseleer et al., 2000; Tippens and Lee, 2007) were a generous gift from Dr. Françoise Haeseleer (Department of Ophthalmology, University of Washington School of Medicine, Seattle, Washington). Generated and purified from a bacterially expressed CaBP1-S protein (*arrowheads*, Fig. 2A), these anti-CaBP1/CD antibodies recognize all variants. Specificity of the CaBP1/CD antiserum was confirmed by immunoblotting and immunohistochemistry using CaBP1/CD-null mice. A list of primary antibodies is provided in Table 1.

Tissue Preparation

Adult CaBP1 WT, Het and KO mice were first exposed to isoflurane (Terrell, Bethlehem, PA), and then deeply anesthetized with a peritoneal injection of ketamine (50-100 mg/kg). Mouse hearts were intracardially rinsed with 0.1 M phosphate buffer (PB; 0.1 M, pH 7.4) then perfused with 4% paraformaldehyde. The brains were carefully removed, postfixed for 3-4 hours on ice, and then immersed in 15% sucrose (in 0.1 M PB) overnight followed by a 24-hour incubation in 30% sucrose (in 0.1 M PB) at 4°C. Brain sections were cut into 40-µm-thick coronal and sagittal sections collected using the Leica CM-3050-S Cryostat machine, and either used immediately or stored in cryoprotectant solution (30% sucrose, 30% ethylene glycol in 0.1 M PB, pH 7.4) at -20°C.

Double Immunofluorescence Labeling

Brain sections were rinsed three times with phosphate buffered saline (PBS) for 10 minutes before blocking in blocking buffer (BB: 10% normal goat serum (NGS; Jackson Immunoresearch), 0.3 % Triton X-100 in PBS) for 1 hour at room temperature. All primary antibodies were diluted and incubated in BB overnight in 4°C. Sections were rinsed three times for 15 minutes each in

PBS containing 1% NGS and 0.3 % Triton X-100 [washing buffer (WB)]. Free-floating sections were incubated with Alexa Fluor-488 conjugated goat anti-rabbit IgG and Alexa Fluor-546 conjugated goat anti-mouse IgG (1:1000, Invitrogen, Carlsbad, CA) for 1-3 hours at room temperature. The first and second washes were in WB for 15 minutes, and then the remaining washes were in PBS for 15 minutes (four times) and in 0.05 M PB for five minutes.

Sections were mounted onto 25 x 75 x 1.0 mm glass microscope slides (Fisherbrand), and coated with Prolong Gold Antifade Reagent (Life Technologies). The processed tissues were viewed under a confocal laser-scanning microscope (Olympus Fluoview FV1000, Melville, NY). Images were taken using x60 and x100 oil immersion objectives with numerical apertures of 1.45 and 1.30, respectively. CaBP1/CD-labeling was captured after setting fluorescent signals from CaBP1 KO sections as the threshold. In double labeling experiments, images were acquired independently, and scanned using a step size from 0.15 to 0.4 μm. A total of 18-30 optical sections were collected. Single optical slices were compiled into one image (Z-stacked) using the Fluoview software. Colocalization was analyzed using single optical sections. Images were later transferred to Adobe Photoshop for brightness and contrast adjustment.

Immunoperoxidase Labeling

Free-floating sections underwent immunoperoxidase staining following the standard 3,3'-diamonibenzadine (DAB)/nickel immunperoxidase (Vectastain, Burlingame, CA) protocols in Tris-buffered saline (TBS). Sections were rinsed three times in TBS for 10 minutes each at room temperature before blocking endogenous peroxides with 0.3% hydrogen peroxide (H_2O_2), and rinsed in TBS. Similar to our immunohistochemistry methods, sections were blocked in BB for 1 hour at 4°C, and submerged in BB containing primary antibodies (polyclonal anti-CaBP1/CD rabbit diluted to 1:15,000), and incubated overnight at 4°C. The following day, sections were

washed three times in TBS for 10 minutes each followed by a secondary antibody incubation with donkey anti-rabbit biotinylated antibodies (1:400; Abcam, Cambridge, MA) for one hour at room temperature. Brain sections were rinsed three times in TBS for 10 minutes each.

Prior to adding DAB, sections were incubated with an avidin-biotin-peroxidase complex (ABC-Elite, Vectastain) mix for 30 minutes, and thoroughly rinsed three times with TBS for 10 minutes. Sections were then transferred and washed in a solution containing DAB for 7 minutes before mounting onto gelatin-subbed slides (Southern Biotech, Birmingham, AL), and underwent multiple dehydration steps using 75%, 95% and 100% ethanol and xylene solutions. After the last dehydration step, the processed tissues were coverslipped with DPX mountant (Gallard Schlesinger Industries, Plainview, NY). DAB labeled sections were viewed under an Olympus BX53 microscope using x2, x20 non-oil and x60 oil immersion objectives with a numerical aperture of 0.08, 0.50 and 1.35.

Cell Culture and Transfection

Human embryonic kidney cells, HEK293T (ATCC, Manassas, VA), were grown and maintained in Dulbeco's modified Eagle's medium (Life Technologies) with 10% Fetal Bovine Serum (Atlanta Biologicals, Lawrenceville, GA), penicillin and streptomycin (Life Technologies), and held in a humidified atmosphere at 37°C and 5% CO_2. Once cells have reached 70-80% confluence, cells were transfected with plasmid DNA using a Gene Porter reagent (Genlantis, San Diego, CA).

CaBP1 and CD Protein Expression in HEK293T Cells and Cell Lysate Preparation

HEK293T cells plated on 35 mm dishes were transfected with 2.0 μg of CaBP1 plasmids. One day later, cells were rinsed and suspended with Versene Solution (Life Technologies), and

pelleted at 800 x g for 5 min. (4°C). After removal of supernatant, cells were homogenized using ice-cold RIPA buffer (150 mM sodium chloride, 1% Triton X-100, 0.5% sodium deoxycholate, 0.1% sodium dodecyl sulfate (SDS), 50 mM Tris, pH 8.0) and sterile pellet pestles (Kimble Chase Kontes, Vineland, NJ). Supernatant was collected after spinning homogenates at 16,200 x g for 15 min. (4°C), and either used immediately or aliquoted and stored at -20°C.

Crude Cytosol/Membrane Prep Protocol

After deep sedation of mice, brains were dissected out, and rinsed in 0.5 ml cold HEPES Buffer (HB: 0.32 M sucrose, 10 mM HEPES, pH 7.4, 2 mM EDTA, pH 8, EDTA-free protease inhibitor mix cocktail tablet; Roche, Indianapolis, IN). Brain regions were separated, and transferred to a 1.5 ml microcentrifuge tube. Brain tissue was homogenized using a plastic pestle and pellet pestle cordless motor (Kimble Chase Kontes) until tissue lysates appeared homogenous. To extract the nuclear pellet (P1), brain lysate underwent a low speed spin at 1000 x g for 15 minutes (4°C) using Microcentrifuge 5415R (Eppendorf, Westbury, NY). The resulting supernatant of P1 (S1) was transferred to a polycarbonate centrifuge tube (Beckman, Brea, CA). Using a Beckman rotor TLA 120.2 (Beckman), crude membrane pellet (P2) was isolated at 100,000 x g for 15 minutes (4°C) in a Beckman's Optima TLX Ultracentrifuge (Beckman). Suspended with 0.5 ml of HB, P2 was re-pelleted after spinning at 200,000 x g for 15 minutes (4°C). P2 was suspended using 0.1 ml of HEPES lysis buffer (HLB: 50mM HEPES, pH 7.4, 2mM EDTA, Roche's EDTA-free protease inhibitor cocktail mix). Total protein concentration was measured using a BCA Protein Assay (Thermo Scientific, Rockford, IL). 30-50 μg of crude cytosol and membrane fractions were run on polyacrylamide gels, while the remaining fractions were aliquoted, and stored at -80°C.

Immunoblotting

Freshly prepared protein samples were prepared by adding appropriate volumes of dH_2O and reducing agent, lithium dodecyl sulfate, pH of 8.4 (Life Technologies). The samples were heated at ~95°C for 15 minutes, and loaded into NuPage Novex 10% Bis-Tris wells (Life Technologies). These polyacrylamide gels were run at 100 volts for 1.5-2 hours, and transferred onto a nitrocellulose membrane (BioRad, Hercules, CA) at 80 volts for 3 hours. Blots were blocked in 3-5 ml of 3% milk and TBST (0.1% Tween20 in TBS) for 1 hour at room temperature, and then incubated with primary polyclonal antibody, anti-CaBP1/CD (1:1000 for transfected HEK293T cell lysates and 1:4000 for brain fractions), for 1 hour at room temperature. After being rinsed three times in TBST, immunoblots were incubated with secondary antibody horseradish peroxidase anti-rabbit (1:4000; Jackson Immunoresearch) for 45 minutes at room temperature. Blots were again rinsed three times with TBST before applying chemiluminescent substrates (Thermo Scientific), and exposed to an autoradiography film (Denville).

Table 1. List of Primary Antibodies used for immunohistochemistry (IHC) and western blot (WB) analysis

Antigen	**Immunogen**	**Species**	**Source (catalog no.)**	**Working dilution IHC/WB**
CaBP1	Mouse CaBP1-S aa 25-227	Rabbit polyclonal	F. Haeseleer	1:500 / 1:1000 cell lysates, 1:4000 brain sections
Calbindin-D-28K	Purified bovine kidney calbindin-D-28K	Mouse monoclonal	Sigma Aldrich (C9848)	1:6000
Calretinin	Recombinant rat calretinin	Mouse monoclonal	Millipore (MAB1568)	1:500
$K_v1.2$	Human $K_v1.2$ aa 428-499	Mouse monoclonal	UC Davis/NIH NeuroMab Facility (75-008)	1:400
Parvalbumin	Purified frog muscle parvalbumin	Mouse monoclonal	Sigma Aldrich (P3088)	1:500
Tyrosine hydroxylase	Tyrosine hydroxylase from a rat pheochromocytoma	Mouse monoclonal	Millipore (MAB5280)	1:1000

CHAPTER III.

RESULTS

Generation of CaBP1/CD-deficient Mice

We studied the expression and localization of CaBP1/CD in the mouse brain by RT-PCR and immunohistochemical methods, respectively. To ensure the specificity of our reagents for these experiments, we generated mice that lack expression of CaBP1/CD. We constructed a targeting construct which, upon homologous recombination of the inserted DNA sequence, would cause expression of a neomycin resistance gene and mCherry fluorescent protein in place of exon 1a and 1b of the mouse CaBP1/CD gene (Fig. 1A). 129/SvEv embryonic stem (ES) cells were electroporated with this CaBP1/CD targeting construct and recombinant ES cells that were neomycin-resistant and contained the mCherry sequence were detected by PCR and microinjected into the blastocysts of wild-type C57/Bl6 mice. We confirmed the mutant allele had transferred into the germ-line of chimeric mice by PCR of genomic DNA (Fig. 1B-C). We observed a 419 base pair (bp) PCR product corresponding to the mutant allele only in heterozygous and KO mice (+/-, CaBP1 Het; -/-, CaBP1 KO; Fig. 1B). The WT allele (392 bp fragment from exon 1a) was detected in WT (+/+; CaBP1 WT) and heterozygous mice. These results indicated successful incorporation of the mutant allele by homologous recombination.

We further confirmed the disruption of CaBP1/CD expression in CaBP1 KO mouse by RT-PCR. cDNA was synthesized from isolated brain RNA of CaBP1 WT, Het and KO mice. To validate the specificity of the CaBP1 and CD primers, we used CaBP1 and CD plasmids, and observed the expected PCR product from each reaction (Fig. 1B). The amplification of CaBP1/CD variants was only detected in WT and Het mice (Fig. 1C). Despite the lack of CaBP1 PCR products in the KO lane, GAPDH products were amplified in WT, Het and KO mouse indicating

that the total cDNA inputs were relatively the same. Taken together, these results show that CaBP1 KO mice lacked expression of CaBP1 and CD.

Comparison of CaBP1/CD Isoforms

CaBP1-L differs from CaBP1-S in that it possesses a 60-amino acid insertion (aa 16-75), which results in ~27 kDa protein product. CaBP1-S remains to be the smallest of the three isoforms with a molecular weight of ~19 kDa. CD, being the longest of the three isoforms, has an N-terminal region distinct from that of other CaBPs. Two protein products have been reported for CD (33 kDa (CD-S) and 36 kDa (CD-L)) (Seidenbecher et al., 1998). In order to determine the relative protein levels of CaBP1 and CD, we probed for each isoform by immunoblotting methods using polyclonal anti-CaBP1/CD rabbit antibodies [UW72 (Haeseleer et al., 2000)] generated against a sequence common to all variants (*arrowheads*, Fig. 2A).

By western blotting, our CaBP1/CD antibody recognized all three variants in lysates of HEK293T cells transfected with each isoform (Fig. 2B). These antibodies detected CD (especially CD-S) in the cytosol and membrane fractions of WT mouse brain (lanes 5 and 6; Fig. 2C). However, we did not detect CaBP1-S and -L proteins in either crude membrane or cytosol fractionations (Fig. 2C). These results suggested that CD may be more highly expressed in the brain compared to CaBP1-S and -L.

To follow up on this possibility, we performed qRT-PCR assays using RNA isolated from three brain regions. Using CaBP1 and CD-specific probes designed by TaqMan (Life Technologies), the relative quantity (RQ) values of CaBP1/CD RNA levels were measured. Based on the RQ values, CD expression was higher in the cerebral cortex (Ctx) compared to the cerebellum (C) or hippocampus (Hc) (Fig. 3A). CaBP1 was significantly greater in the cerebellum than the hippocampus (Fig. 3B), but detected at much lower levels than CD in each brain region

examined. Therefore, CD appears to be the dominant CaBP1/CD variant expressed in the brain at the transcript and protein level.

Previous studies suggest that the two variants of CD (CD-S and CD-L) are due to a conformational change induced by phosphorylation, which causes a shift in the electrophoretic mobility of the protein (Laube et al., 2002; Seidenbecher et al., 1998). However, there is a second methionine residue upstream of the methionine that would initiate translation of CD-S. Therefore the 36 kDa could correspond to a larger protein resulting from the upstream alternative site for translation (CD-L, Fig. 1A). CD-L would include an additional 53 amino acids in its sequence compared to CD-S. To test this possibility, we generated cDNA expression constructs for mouse CD that would contain either of these translation start sites (CD-S and CD-L) and expressed them in HEK293T cells. By western blotting, the molecular weight of CD-L expressed in HEK293T cells (lane 4) was similar to the 36 kDa from mouse brain lysates (lanes 5-6; Fig. 2C). This result suggests that the upstream alternate translation start site, rather than phosphorylation, could account for the larger protein detected by CaBP1/CD antibodies in mouse brain.

Distribution of CaBP1/CD Labeling in the Mouse Brain

To study the localization of CaBP1/CD in the murine brain, we performed immunoperoxidase labeling in coronal and sagittal brain sections from CaBP1 +/+ (wild-type) and +/- (heterozygous) mice. Throughout the brain, intense CaBP1/CD immunoreactivity (IR) was concentrated in brain regions with a laminar organization like the olfactory bulb, cerebral cortex, hippocampus or cerebellum (Fig. 4A). Intense CaBP1/CD IR was also visualized in the brain stem and piriform cortex (Fig. 4A). Immunoperoxidase labeling was specific in that it was observed in WT (Fig. 4A) but not CaBP1 KO brain sections (Fig. 4B).

Distribution of CaBP1/CD varied along the rostral-caudal axis of the forebrain. In the cerebral cortex, strong CaBP1/CD IR was observed in principal cell bodies and dendrites in the piriform and somatosensory cortices (Fig. 4C-D). Furthermore, CaBP1/CD antibodies more strongly labeled somatosensory cortical layers II/III compared to layers V/VI (Fig. 4C-D, 5D). However, CaBP1/CD IR was generally consistent in intensity throughout the layers of the piriform cortex (Fig. 4C-D). In the hippocampus, we observed CaBP1/CD IR primarily in CA3 neurons (Fig. 4C, 5A-B), but very faint CaBP1/CD IR was found in CA1 and CA2 regions (*arrow*, Fig. 5A). In contrast to the strong localization of other Ca^{2+} binding proteins, such as parvalbumin and calbindin D-28k (Kawaguchi et al., 1995; Tepper and Bolam, 2004), CaBP1/CD IR was very weak in the striatum.

We also examined the localization of CaBP1/CD in the substantia nigra. One of the known targets of CaBP1/CD, $Ca_v1.3$ Ca^{2+} channels, is highly expressed in tyrosine hydroxylase (TH)-expressing dopaminergic neurons in the substantia nigra pars compacta (SNc), where they may contribute to spontaneous neuronal firing and the progression of Parkinson's disease (Chan et al., 2007). Double immunofluorescence labeling was performed on adult CaBP1 WT coronal brain sections using polyclonal anti-CaBP1/CD rabbit and monoclonal anti-TH mouse antibodies. TH-positive cells (magenta) in the SNc were CaBP1/CD-negative (Fig. 4E-G). While these catecholaminergic cells lacked CaBP1/CD labeling in the SNc, CaBP1/CD (green) immunolocalized preferentially in substantia nigra pars reticulata (SNr) neurons where mainly PV-positive GABA-ergic neurons reside (Zhou and Lee, 2011). These results show that within the substantia nigra, CaBP1/CD may regulate effectors in GABA-ergic neurons, but is not a likely modulator of $Ca_v1.3$ channels in dopaminergic neurons.

CaBP1/CD Labeling in the Hippocampus and Cerebral Cortex

Within the hippocampal formation, CaBP1/CD labeling was particularly intense in the CA3 region and in the hilus of dentate gyrus (DG) (Fig. 5A-C). In the CA3 region, mainly pyramidal cell soma and dendrites were labeled, but some neurons scattered throughout the stratum oriens and radiatum also exhibited strong CaBP1/CD labeling (Fig. 5A-B). To characterize these CaBP1/CD-positive cells using neurochemical markers, we performed double immunofluorescence labeling on adult CaBP1 WT mouse brain sagittal sections using CaBP1/CD (green) and anti-parvalbumin (PV) or anti-calretinin (CR) antibodies (magenta). Our results reveal only moderate overlap between PV- and CaBP1/CD-positive neurons in the stratum oriens and radiatum. Rather, PV-containing axons innervated CaBP1/CD-expressing CA3 neurons as some formed synaptic contact with CaBP1/CD-expressing neurons (*arrowhead*, Fig. 6C).

In the CA1 region, some CaBP1/CD-expressing pyramidal cells were PV-positive (*arrow*, Fig. 6D-F) while some were not (*arrowhead*, Fig. 6D-F). In contrast to the staining we observed in the CA regions, we detected relatively weak CaBP1/CD staining in the hilus (Fig. 4D, 5G-I). Although the granule cells of the dentate gyrus lacked CaBP1/CD staining, moderate labeling was observed in the hilus (Fig. 4C), but CR-expressing hilar mossy cells (Fujise et al., 1998) were CaBP1/CD negative (Fig. 6G-I).

CaBP1/CD distribution varied throughout the cortical layers. Layers II/III and V/VI of the somatosensory cortices showed intense CaBP1/CD IR compared to layers I and IV (Fig. 4C-D). In the somatosensory cortical layer V/VI, the majority of CaPB1/CD staining is concentrated predominantly in cell bodies and apical proximal dendrites (Fig. 5D-F). Dendritic processes of pyramidal cells extending from layers V/VI to layers II/III exhibited intense CaBP1/CD labeling

(*arrow*, Fig. 5F). Taken together, these results largely confirm previous descriptions of CaBP1/CD localization in neurons that may regulate learning, memory and cognitive functions.

CaBP1/CD Labeling in the Cerebellum

We detected strong CaBP1/CD labeling in cerebellar interneurons (basket and stellate cells) (*arrow*) as well as fibers (*arrowhead*) residing in the molecular layer (M) (Fig. 7A). More than 50% of the CaBP1/CD-expressing interneurons (green) overlapped (*arrow*) with PV-containing neurons (magenta) in the molecular layer (Fig. 7I-K) by double immunofluorescence staining. The purkinje layer (P) and interneurons of the granule layer (G) displayed very weak labeling (Fig. 7A-B).

In order to investigate the identity of these CaBP1/CD-containing cells in the purkinje layer (P), we performed double immunofluorescence analysis using CaBP1/CD and anti-CB antibodies, a Ca^{2+} binding protein localized in Purkinje cell somas, dendrites, and axons (Iacopino et al., 1990; Ishikawa et al., 1995; Schwaller et al., 2002). Purkinje cell somas (asterisk) were completely void of CaBP1/CD staining (green) as CaBP1/CD failed to colocalize with CB (magenta; Fig. 7C-E). Rather the puncta pattern observed in the purkinje layer (P) appeared perisomatic.

CaBP1/CD labeling was absent in Purkinje cell bodies (*arrow*, Fig. 7C), but instead, localized near the axon initial segment (AIS). This specialized structure is known as the pinceau formation, a compartment shaped by basket cell axons in the molecular layer (M) wrapping around the AIS of cerebellar Purkinje cells. As high levels of *Shaker-type* potassium channels, $K_v1.2$, have been reportedly localized in these specialized structures (Iwakura et al., 2012), the overlap between CaBP1/CD and $K_v1.2$ strongly suggest CaBP1/CD is localized in the cerebellar pinceau formations (*arrow*, Fig. 7F-H). CaBP1/CD is the only known CaBP member confined in these presynaptic

GABA-ergic compartments, which broadens our understanding on CaBP1/CD-mediated Purkinje-cell regulation, and furthermore, modulation of postsynaptic Ca^{2+} signaling in inhibitory neurons.

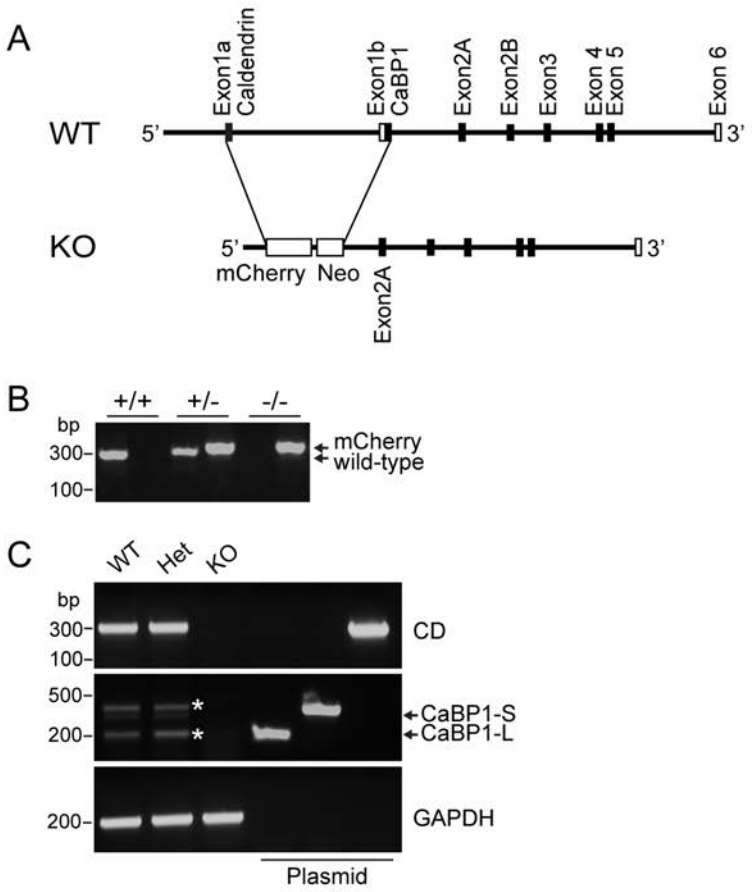

Figure 1. Generation of CaBP1/CD-deficient mouse. *A,* Disruption of exon 1 in CaBP1 KO mouse with mCherry and neomycin cassette sequences. *B,* Wild-type allele was present in CaBP1 +/+ and +/-, and mutant allele (mCherry) was detected only in CaBP1 +/- and -/- genomic DNA. *C*, Using RT-PCR, CaBP1 and CD primers amplified CaBP1 variants from CaBP1 WT and Het brain cDNA. GAPDH was used as loading control in RT-PCR experiments. N = 3 adult mice (P40-134) CaBP1 wild-type, +/+ or WT; heterozygous, +/- or Het; knock-out, -/- or KO; caldendrin, CD; CaBP1 short and long, CaBP1-S and -L.

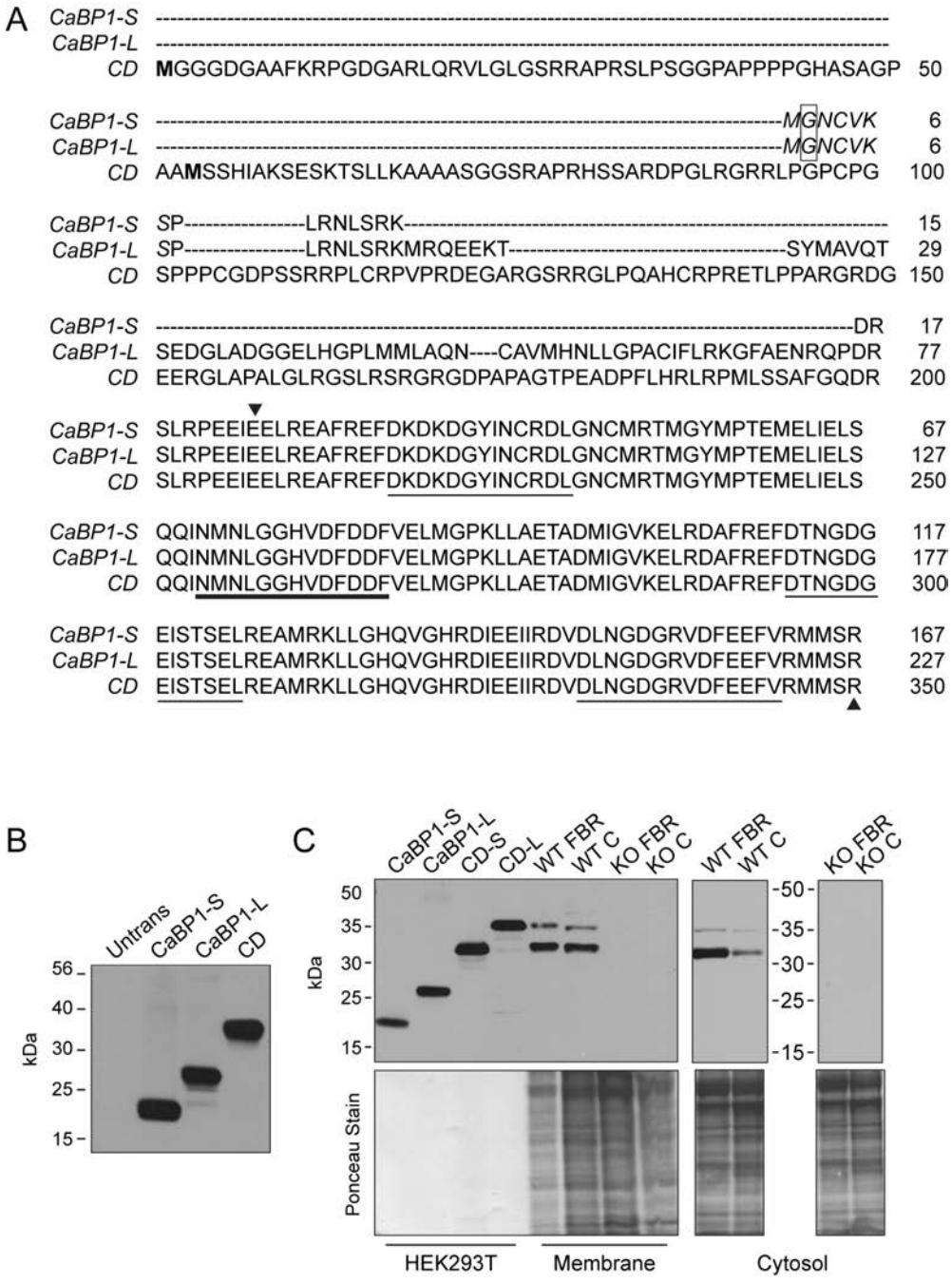

Figure 2. Specificity of CaBP1/CD antibody determined by immunoblotting. *A,* Sequence alignment of CaBP1 variants using Clustal Omega Multiple Sequence Alignment. Isoforms encode 4 EF-hand motifs (*underlined*) while EF2 (*bold, underlined*) is nonfunctional. An N-myristoylation site (*box*) is present in CaBP1-S and -L, and two potential start sites (*bold*) in CD. CaBP1/CD antibody was generated using a truncated CaBP1-S protein (aa 25-227; *arrowhead*). *B-C*, CaBP1/CD antibody recognized all variants in transfected HEK293T cell lysates, and only CD-S and -L in crude WT membrane (50 μg) and cytosol (30 μg) fractions. N = 4 adult mice (P40-55); CD short and long, CD-S and -L; wild-type, WT; knock-out, KO; forebrain, FBR; cerebellum, C.

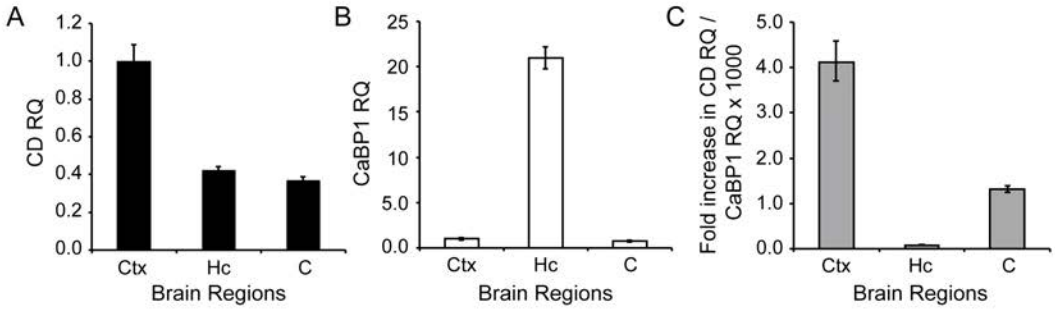

Figure 3. CaBP1 and CD mRNA expression in the mouse brain. RNA from the indicated brain regions of one-month old mice was reverse-transcribed and quantitative real-time PCR (qPCR) was performed using Taqman primer/probe sets specific to caldendrin or CaBP1. GAPDH was used as an endogenous reference. Data are displayed as the relative quantity (RQ) of caldendrin compared to CaBP1 transcripts (*C*) or the RQ of CD (*A*) and CaBP1 (*B*) transcripts relative to levels in the cortex. Error bars represent the minimum and maximum RQ values calculated based on a 95% confidence interval of threshold cycle values. N = 3-4 mice, data averaged from 3 separate qPCR experiments. Cerebral cortex, Ctx; hippocampus, Hc; cerebellum, C.

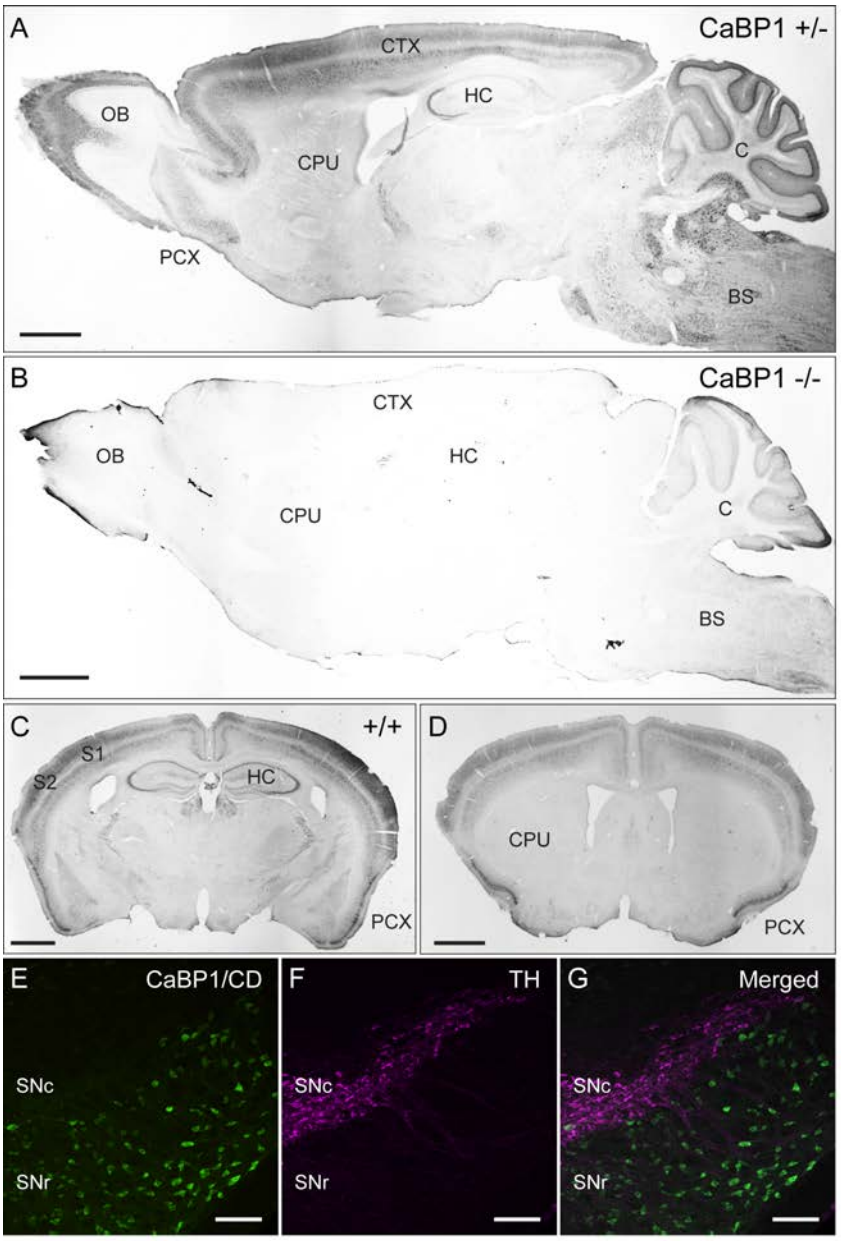

Figure 4. Distribution of CaBP1/CD variants in the mouse brain. Sagittal view of CaBP1 +/- (*A*) and -/- (*B*) brain sections. CaBP1/CD-IR detected in brain regions with a laminar organization such as the OB, CTX, HC, C and PTX in adult CaBP1 +/+ and +/- mice. A subset of neurons in the BS were also immunopositive (*A*, *C-D*). Rostral (*C*) and mid-caudal (*D*) regions. S1 and S2 cortices were highly CaBP1/CD-IR compared to other cortical regions (coronal view). Very weak CaBP1/CD labeling in the striatum (CPU; *D*) and SNc (*E-G*). CaBP1/CD (green) does not colocalize with TH-expressing dopaminergic neurons (red) in the SNc, but highly localized in the SNr (coronal view). Immunofluorescence viewed under a laser scanning confocal microscope, Olympus FV1000. N = 3-6 mice (P40-100). Cerebral cortex, Ctx; cerebellum, C; hippocampus, Hc; olfactory bulb, OB; piriform cortex, Ptx; somatosensory cortices, S1; secondary somatosensory cortex, S2; caudate-putamen, CPu; substantia nigra pars compacta and pars reticulata, SNc and SNr; tyrosine hydroxylase, TH. Scale bar 1 mm in *A-D*, and 50 μm in *E-F*.

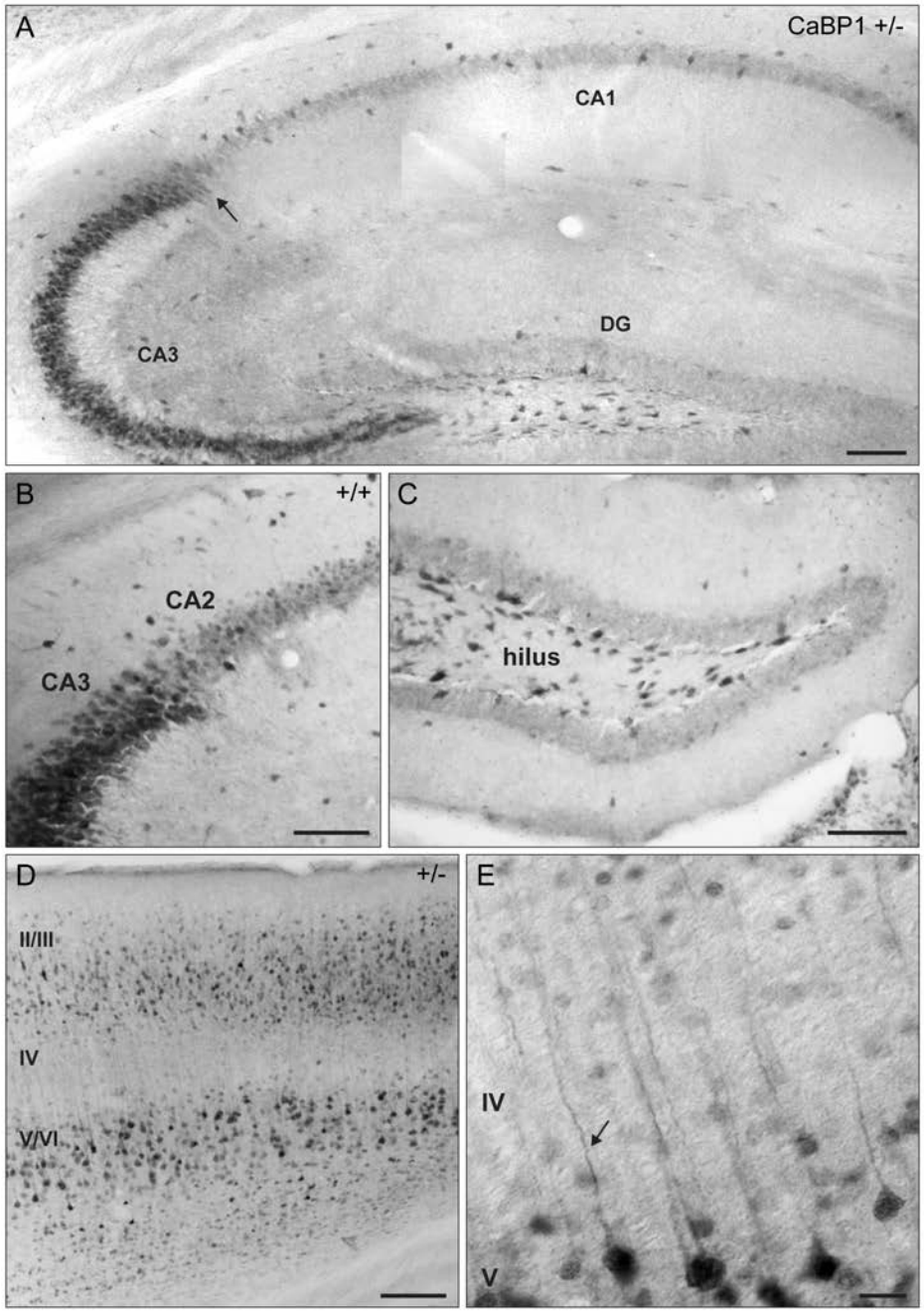

Figure 5. CaBP1/CD exhibits somato-dendritic localization in a subset of neurons. *A-B*, Strong CaBP1/CD-IR detected in the somato-dendritic compartments of hippocampal CA3 neurons (*arrow*) and pyramidal cells of somatosensory cortical layers II/III and V/VI (*D-E*) in CaBP1 +/+ and +/- mouse brain (sagittal view). *E*, In apical dendritic processes, CaBP1/CD localization (*arrow*) extended from cortical layer V to layers II/III. Moderate CaBP1/CD labeling in the hilus (*A, C*). N = 3-6 mice (P40-100). Hippocampal cornu ammonis regions, CA1, 2, 3; dentate gyrus, DG. Scale bars, 100 μm in *A-D*, and 20 μm in *E*.

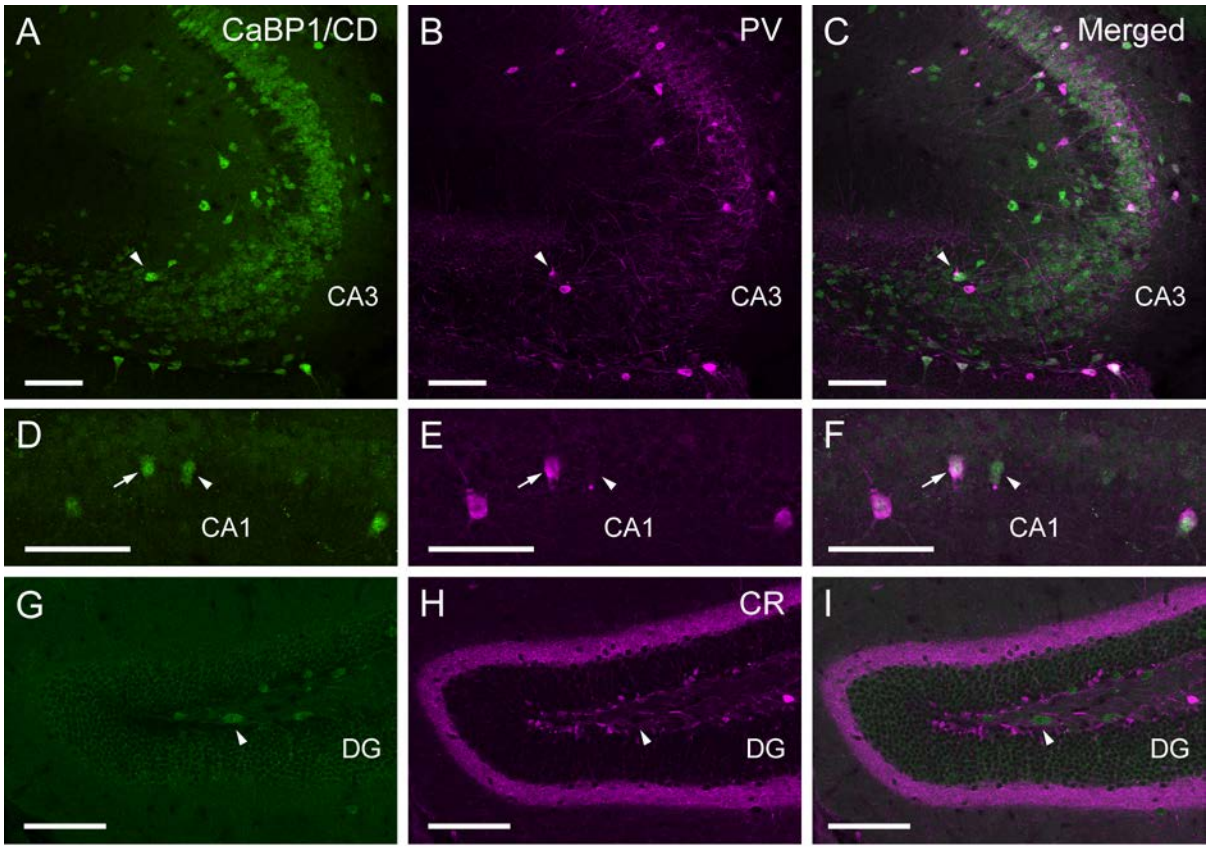

Figure 6. Moderate overlap of CaBP1/CD and PV or CR. *A-C*, Modest overlap of CaBP1/CD and parvalbumin (PV)-positive interneurons in the hippocampal CA3 region. *D-F*, Few CaBP1/CD-containing CA1 neurons express PV (*arrow*; CaBP1/CD only, *arrowhead*). G-I, Lack of CaBP1/CD staining in calretinin (CR)-containing hilar cells. Moderate CaBP1/CD staining in CR-containing mossy cells (*arrowhead*). N = 3-5 adult mice (P40-100). Dentate gyrus, DG; scale bars, 100 μm.

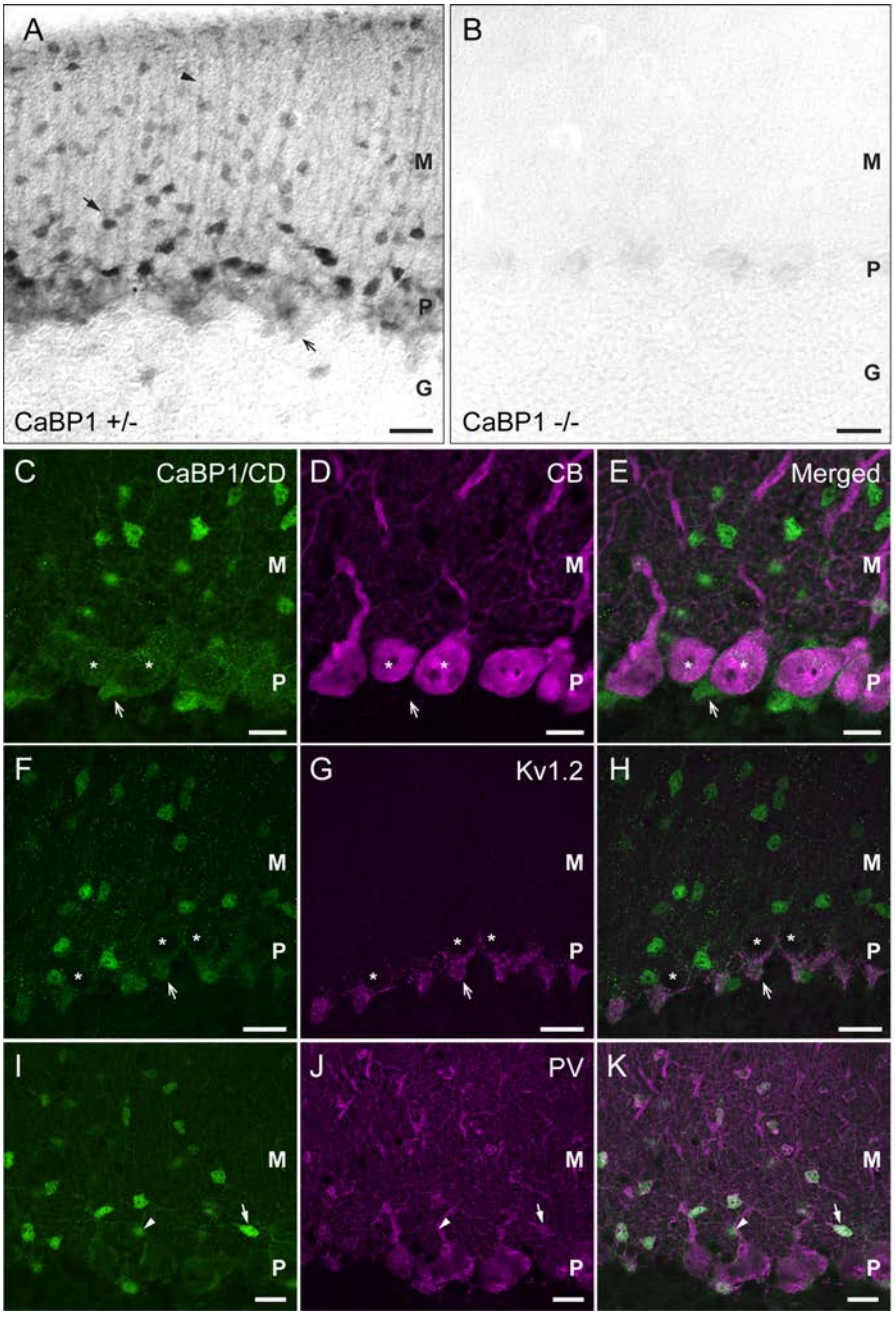

Figure 7. CaBP1/CD localization in the mouse cerebellum. CaBP1/CD localized in cerebellar neurons (*arrow*) and fibers of the molecular layer (*arrowhead*), and found at the base of Purkinje cells (asterisk) in CaBP1 +/- (*A*), but not CaBP1 -/- (*B*) sections (sagittal view). *C-E*, CaBP1/CD is detected at low levels in calbindin-D-28K (CB)-positive Purkinje neurons (*asterisk*), but is intensely localized in pinceaux formations (*arrow*). *F-H*, $K_v1.2$ and CaBP1/CD overlap in pinceaux formations. *I-K*, Few CaBP1/CD-containing interneurons are PV-positive (*arrow*; CaBP1/CD only, *arrowhead*). N = 3-6 adult mice (P40-100). Molecular layer, M; purkinje layer, P; granule layer, G. Scale bars, 100 μm in *A-B*, 20 μm in *C-K*.

CHAPTER IV.

DISCUSSION

Our studies provide a framework for understanding of CaBP1/CD-mediated Ca^{2+} signaling in the murine central nervous system. Among the Ca^{2+} sensor protein members, CaBP1/CD is most similar to CaM in the murine brain (Haeseleer et al., 2000; McCue et al., 2010; Mikhaylova et al., 2006), but the precise role of these CaM-like proteins in neuronal Ca^{2+} signaling is poorly understood. Our findings allow us formulate hypotheses regarding the functional significance of CaBP1/CD in the mouse brain, and to test these hypotheses using our CaBP1 KO mouse.

We observed heterogeneous labeling of CaBP1/CD in regions with a laminar organization. Additionally, CaBP1/CD signals were found in both membrane and cytosol fractions with CD-S being the predominant variant expressed in the mouse brain. High RQ values of CD in the cerebral cortex and hippocampus may reflect the importance of CD in the brain functions involved in higher processing and synaptic plasticity. CD is abundantly found in the postsynaptic density of excitatory synapses formed by principal neurons (Laube et al., 2002; Seidenbecher et al., 1998). Our data strongly suggest that CaBP1/CD localizes to both excitatory and inhibitory neurons, and interneurons, extending the possible roles CaBP1/CD has in the brain.

Possible Roles of CaBP1/CD in Neurons

Previous work has shown that CaBP1/CD colocalizes with $Ca_v1.2$ L-type Ca^{2+} channels in neurons, where it may regulate L-type Ca^{2+} signals (Tippens and Lee, 2007; Zhou et al., 2005). This preferential localization of CaBP1/CD in the cell soma, dendrites and dendritic spines of pyramidal cells matches previous descriptions of the localization of $Ca_v1.2$ channels in hippocampal and cerebral cortical pyramidal cells (Hell et al., 1993; Westenbroek et al., 1990). Clustered in the dendrites, dendritic spines (Davare et al., 2001; Hell et al., 1993; Obermair et al.,

2004; Tippens and Lee, 2007), and soma of principal neurons (Westenbroek et al., 1990), $Ca_v1.2$ channels localize to subcellular regions, much as CaBP1/ CD does. Our findings strongly suggest that CaBP1/CD regulates postsynaptic neuronal Ca_v1 channels, which in turn, influences L-type dependent processes such as gene transcription and L-type-dependent long-term potentiation or depression (LTP and LTD).

Mossy fibers from granule cells of the DG form synapses with CA3 pyramidal neurons. At these synapses, postsynaptic Ca_v1 Ca^{2+} influx through L-type Ca^{2+} channels and Ca^{2+} release from inositol 1,4,5-trisphosphate receptor-sensitive intracellular stores produces a distinct form of long-term depression (LTD) in the hippocampus (Lei et al., 2003). It is tempting to speculate that CaBP1/CD is involved in this form of LTD due to its known interaction with $Ca_v1.2$ channels (Tippens and Lee, 2007; Zhou et al., 2004).

With respect to known effects of CaBP1/CD in modulating L-type channel Ca^{2+}-dependent inactivation (CDI), previous work showed moderate level of CDI in thalamocortical (Meuth et al., 2002), and neocortical pyramidal neurons (Stewart and Foehring, 2001). The combined effect of CaBP1/CD and other Ca_v1-mediated regulators localized in the somato-dendritic regions may contribute to this intermediate level of CDI, which may diversify post-synaptic Ca^{2+} signaling in a subpopulation of neurons.

CD-S (33-kDa) is the Main CaBP1/CD Variant

Varying RNA and protein expression levels of CaBP1 and CD in the cerebral cortex, cerebellum, and hippocampus suggest that these CaBP1/CD isoforms are differentially regulated. Previous studies have led to the proposal that CD is the predominant CaBP1/CD splice variant expressed in the murine brain (Haeseleer et al., 2000; Laube et al., 2002). We demonstrated a similar outcome by qRT-PCR and immunoblotting methods (Fig. 2-3). CD exhibited higher RQ

values relative to both CaBP1-S and -L in all three regions. In addition, previous studies have shown that both CD-S and -L coimmunoprecipitate with $Ca_v1.2$ in rat brain (Tippens and Lee, 2007). IR bands corresponding to CaBP1-S and -L could not be detected by western blotting from either rat or mouse brain. Differential intensities of IR bands (33- and 36-kDa) were exhibited in brain, especially with respect to the shorter isoform. We speculate that CD-S (the 33-kDa isoform) is the major CaBP1/CD variant, a binding partner of a synaptic and nuclear protein, Jacob (Grover and Teyler, 1990).

The 33- and 36-kDa CD isoforms may not localize to the same subcellular regions in the murine brain (Laube et al., 2002; Seidenbecher et al., 1998). Found in both the detergent-soluble and -insoluble particulate fraction, the 33-kDa product was detected at higher levels in these subcellular fractions and in acute hippocampal slices (Seidenbecher et al., 1998), while the 36-kDa isoform was found tightly associated with the cortical cytoskeleton (Laube et al., 2002; Seidenbecher et al., 1998). Their N-terminal domains of the proteins may be necessary for specific tissue types, and for their distinct subcellular localization. CaBP1-S localizes primarily to the plasma membrane and Golgi apparatus, while CaBP1-L localizes mainly to the Golgi and exhibits cytosolic localization (Haeseleer et al., 2000; McCue et al., 2009; McCue et al., 2010).

Based on our results, we hypothesized that the two IR bands corresponding to CD-S and -L are isoforms translated from a single mRNA sequence, by alternative translation initiation (ATI), and not the result of differential phosphorylation. The SAPAP3 isoforms (SAPAP3α and β) are scaffolding proteins highly localized in the postsynaptic density of excitatory neurons, and products of ATI (Chua et al., 2012). This finding led us to speculate that, similar to SAPAP3 isoforms, the CD doublet may be due to several intrinsic features within the 5'-untranslated region (5'-UTR), where short reading frames with start codons (uORF) down-regulate translation

efficiency while also facilitating the synthesis of two distinct isoforms via alternative translation initiation (Chua et al., 2012). With multiple uORFs in its 5'-UTR region, the translation efficiency of CD-L may be less favorable, as we have observed greater levels of the shorter isoform in the mouse brain.

The CD-S and CD-L may have divergent functions. Expressed in both glial and neuronal cells, TREK-2 ($K_{2P}10.1$) belongs to the two-pore domain K^+ channel family (Bang et al., 2000; Gnatenco et al., 2002; Gu et al., 2002; Lesage et al., 2000). In mammalian cells, TREK-2 exhibits two unitary conductance levels (~52 pS and ~220 pS) (Simkin et al., 2008), where the long form of TREK-2 (~60 kDa) yields both the small and large-conductance channel, and the two shorter isoforms (~54 kDa) produce only the small-conductance channel (Honore, 2008; Simkin et al., 2008). Similar to TREK-2 and SAPAP3 isoforms, the 33- and 36-kDa may be generated by ATI, and potentially demonstrate distinct regulatory roles.

Moderate levels of CaBP1-S and -L transcripts were observed only in the rat cerebellum by *in-situ* hybridization (Laube et al., 2002; Seidenbecher et al., 1998). CaBP1-S and -L may be important in other regions such as the retina and pituitary tissues, as CD levels were relatively low (Haeseleer et al., 2000; Landwehr et al., 2003). Their tissue-specific distribution has functional implications on plasticity induction. Since the CaBP1/CD antibodies cannot discriminate CaBP1/CD variants, their distinct localization in the mouse brain remains unclear.

CaBP1/CD Localization in Inhibitory Neurons

CaBP1 and CD are located in a subset of excitatory and inhibitory neurons. Presynaptic regions of cerebellar interneurons in the molecular layer were highly CaBP1/CD-immunopositive. Based on their localization, these interneurons are likely to be inhibitory GABA-ergic stellate and basket cells (Deisseroth et al., 2003; Seidenbecher et al., 1998).

Our double immunofluorescence labeling results of $K_v1.2$ and CaBP1/CD revealed that the pinceau formation, which is formed by GABA-ergic basket cells (BC) at the AIS of Purkinje cells (PC) (Iwakura et al., 2012), contains CaBP1/CD. CaBP1/CD may regulate PC activity by either of two modes of inhibition. First, BC may contact PC bodies via perisomatic synapses to inhibit/disinhibit PC activity. Second, the BC might induce electrical inhibition on the PC via the pinceau formation, as supported by the structural similarity of the pinceau formation in the teleost Mauthner cell (Iwakura et al., 2012; Nakajima, 1974; Sotelo, 2008; Triller and Korn, 1980). Furthermore, it is highly likely that CaBP1/CD regulates $Ca_v1.3$ signals in these cerebellar interneurons, since $Ca_v1.3$ channels are also localized in presynaptic regions of basket and stellate cells (Chung et al., 2000), and electrophysiological data suggest that $Ca_v1.3$ is a known CaBP1/CD-modulated effector in transfected cells (Yang et al., 2006).

In the SN, SNr neurons are primarily PV-positive GABA-ergic neurons (Zhou and Lee, 2011), and we found these to be strongly immunopositive for CaBP1/CD. CaBP1 and CD may regulate L-type dependent activation of transient receptor potential (TRP) channels or other target effectors in the SNr such as TRP channels based on its inhibitory effect on TRPC5 channels in Xenopus oocytes (Kinoshita-Kawada et al., 2005). These SNr neurons induce short latency inhibition of neurons (Chevalier et al., 1981; Hikosaka and Wurtz, 1983), which is important for inhibiting or disinhibiting neurons in the motor thalamus, and perhaps for regulating SNr and SNc neurons. SNr neurons exhibit spontaneous activity transduced by Ca_v channels (Zhou and Lee, 2011).

Based on the localization in the hippocampal CA3 stratum radiatum, these CaBP1/CD-expressing neurons are likely to be interneurons. Interneurons in the CA3 stratum radiatum exhibit a distinct form of long-term plasticity, a form of NMDA-independent interneuron LTD (iLTD)

(McBain and Fisahn, 2001). iLTD is induced by high-frequency stimulation of association inputs onto CA3 stratum radiatum interneurons (Laezza et al., 1999) or of mossy fiber inputs onto stratum lucidum interneurons (Toth et al., 2000), which preferably shifts the excitation-inhibition balance towards excitation in the mossy fibre-CA3 system (McBain and Fisahn, 2001). Despite the difficulty of characterizing these hippocampal interneurons using neurochemical markers, we are interested in studying the potential role of all variants in this novel form of synaptic plasticity using electrophysiological recordings on CaBP1 KO hippocampal slices.

CHAPTER V.

CONCLUSION

Understanding how spatially Ca^{2+} signals are regulated will require a detailed knowledge of the Ca^{2+} sensors involved. We observed distinct localization of CaBP1/CD in the postsynaptic somato-dendritic compartments and presynaptic regions of neurons, where these variants may mediate synaptic activity and other cellular responses. Altered distribution of CaBP1/CD-IR was reported in postmortem brains of chronic schizophrenics (Bernstein et al., 2007; McCue et al., 2010). Changes in CaBP1/CD distribution have also been observed in kainate-induced seizures in rats, where CaBP1/CD translocates to the postsynaptic density following epileptic seizures (Bernstein et al., 2007; Smalla et al., 2003). Unfortunately, the involvement of CaBP1/CD in the pathophysiology of these diseases, and the significance of CaBP1 and CD in neurons are not clearly understood. As the list of CaBP1/CD-mediated effectors expands, we hope to address the physiological impact of these variants in the mammalian central nervous system by utilizing the CaBP1 KO mouse.

REFERENCES

Babu YS, Sack JS, Greenhough TJ, Bugg CE, Means AR, Cook WJ. 1985. Three-dimensional structure of calmodulin. Nature 315(6014):37-40.

Bang H, Kim Y, Kim D. 2000. TREK-2, a new member of the mechanosensitive tandem-pore K+ channel family. The Journal of biological chemistry 275(23):17412-17419.

Bernstein HG, Sahin J, Smalla KH, Gundelfinger ED, Bogerts B, Kreutz MR. 2007. A reduced number of cortical neurons show increased Caldendrin protein levels in chronic schizophrenia. Schizophr Res 96(1-3):246-256.

Chan CS, Guzman JN, Ilijic E, Mercer JN, Rick C, Tkatch T, Meredith GE, Surmeier DJ. 2007. 'Rejuvenation' protects neurons in mouse models of Parkinson's disease. Nature 447:1081-1086.

Cheung WY. 1980. Calmodulin plays a pivotal role in cellular regulation. Science 207(4426):19-27.

Chevalier G, Deniau JM, Thierry AM, Feger J. 1981. The nigro-tectal pathway. An electrophysiological reinvestigation in the rat. Brain research 213(2):253-263.

Chua JJ, Schob C, Rehbein M, Gkogkas CG, Richter D, Kindler S. 2012. Synthesis of two SAPAP3 isoforms from a single mRNA is mediated via alternative translational initiation. Scientific reports 2:484.

Chung YH, Shin C, Park KH, Cha CI. 2000. Immunohistochemical study on the distribution of neuronal voltage-gated calcium channels in the rat cerebellum. Brain research 865(2):278-282.

Crivici A, Ikura M. 1995. Molecular and structural basis of target recognition by calmodulin. Annual review of biophysics and biomolecular structure 24:85-116.

Davare MA, Avdonin V, Hall DD, Peden EM, Burette A, Weinberg RJ, Horne MC, Hoshi T, Hell JW. 2001. A beta2 adrenergic receptor signaling complex assembled with the Ca^{2+} channel $Ca_v1.2$. Science 293(5527):98-101.

Deisseroth K, Mermelstein PG, Xia H, Tsien RW. 2003. Signaling from synapse to nucleus: the logic behind the mechanisms. Current opinion in neurobiology 13(3):354-365.

Fujise N, Liu Y, Hori N, Kosaka T. 1998. Distribution of calretinin immunoreactivity in the mouse dentate gyrus: II. Mossy cells, with special reference to their dorsoventral difference in calretinin immunoreactivity. Neuroscience 82(1):181-200.

Gnatenco C, Han J, Snyder AK, Kim D. 2002. Functional expression of TREK-2 K+ channel in cultured rat brain astrocytes. Brain research 931(1):56-67.

Grover LM, Teyler TJ. 1990. Two components of long-term potentiation induced by different patterns of afferent activation. Nature 347(6292):477-479.

Gu W, Schlichthorl G, Hirsch JR, Engels H, Karschin C, Karschin A, Derst C, Steinlein OK, Daut J. 2002. Expression pattern and functional characteristics of two novel splice variants of the two-pore-domain potassium channel TREK-2. The Journal of physiology 539(Pt 3):657-668.

Haeseleer F, Imanishi Y, Maeda T, Possin DE, Maeda A, Lee A, Rieke F, Palczewski K. 2004. Essential role of Ca^{2+}-binding protein 4, a $Ca_v1.4$ channel regulator, in photoreceptor synaptic function. Nat Neurosci 7(10):1079-1087.

Haeseleer F, Imanishi Y, Sokal I, Filipek S, Palczewski K. 2002. Calcium-binding proteins: intracellular sensors from the calmodulin superfamily. Biochem Biophys Res Commun 290(2):615-623.

Haeseleer F, Sokal I, Verlinde CL, Erdjument-Bromage H, Tempst P, Pronin AN, Benovic JL, Fariss RN, Palczewski K. 2000. Five members of a novel Ca(2+)-binding protein (CABP) subfamily with similarity to calmodulin. The Journal of biological chemistry 275(2):1247-1260.

Hell JW, Westenbroek RE, Warner C, Ahlijanian MK, Prystay W, Gilbert MM, Snutch TP, Catterall WA. 1993. Identification and differential subcellular localization of the neuronal class C and class D L-type calcium channel alpha 1 subunits. J Cell Biol 123(4):949-962.

Hikosaka O, Wurtz RH. 1983. Visual and oculomotor functions of monkey substantia nigra pars reticulata. I. Relation of visual and auditory responses to saccades. J Neurophysiol 49(5):1230-1253.

Honore E. 2008. Alternative translation initiation further increases the molecular and functional diversity of ion channels. The Journal of physiology 586(Pt 23):5605-5606.

Iacopino AM, Rhoten WB, Christakos S. 1990. Calcium binding protein (calbindin-D28k) gene expression in the developing and aging mouse cerebellum. Brain research Molecular brain research 8(4):283-290.

Ikura M, Clore GM, Gronenborn AM, Zhu G, Klee CB, Bax A. 1992. Solution structure of a calmodulin-target peptide complex by multidimensional NMR. Science 256(5057):632-638.

Ishikawa K, Mizusawa H, Fujita T, Ohkoshi N, Doi M, Komatsuzaki Y, Iwamoto H, Ogata T, Shoji S. 1995. Calbindin-D 28k immunoreactivity in the cerebellum of spinocerebellar degeneration. Journal of the neurological sciences 129(2):179-185.

Iwakura A, Uchigashima M, Miyazaki T, Yamasaki M, Watanabe M. 2012. Lack of molecular-anatomical evidence for GABAergic influence on axon initial segment of cerebellar

Purkinje cells by the pinceau formation. The Journal of neuroscience : the official journal of the Society for Neuroscience 32(27):9438-9448.

Kawaguchi Y, Wilson CJ, Augood SJ, Emson PC. 1995. Striatal interneurones: chemical, physiological and morphological characterization. Trends in neurosciences 18(12):527-535.

Kinoshita-Kawada M, Tang J, Xiao R, Kaneko S, Foskett JK, Zhu MX. 2005. Inhibition of TRPC5 channels by Ca2+-binding protein 1 in Xenopus oocytes. Pflugers Arch.

Laezza F, Doherty JJ, Dingledine R. 1999. Long-term depression in hippocampal interneurons: joint requirement for pre- and postsynaptic events. Science 285(5432):1411-1414.

Landwehr M, Redecker P, Dieterich DC, Richter K, Bockers TM, Gundelfinger ED, Kreutz MR. 2003. Association of Caldendrin splice isoforms with secretory vesicles in neurohypophyseal axons and the pituitary. FEBS Lett 547(1-3):189-192.

Laube G, Seidenbecher CI, Richter K, Dieterich DC, Hoffmann B, Landwehr M, Smalla KH, Winter C, Bockers TM, Wolf G, Gundelfinger ED, Kreutz MR. 2002. The neuron-specific Ca2+-binding protein caldendrin: gene structure, splice isoforms, and expression in the rat central nervous system. Molecular and cellular neurosciences 19(3):459-475.

Lee A, Westenbroek RE, Haeseleer F, Palczewski K, Scheuer T, Catterall WA. 2002. Differential modulation of Ca(v)2.1 channels by calmodulin and Ca2+-binding protein 1. Nature neuroscience 5(3):210-217.

Lei S, Pelkey KA, Topolnik L, Congar P, Lacaille JC, McBain CJ. 2003. Depolarization-induced long-term depression at hippocampal mossy fiber-CA3 pyramidal neuron synapses. The Journal of neuroscience : the official journal of the Society for Neuroscience 23(30):9786-9795.

Lesage F, Terrenoire C, Romey G, Lazdunski M. 2000. Human TREK2, a 2P domain mechano-sensitive K+ channel with multiple regulations by polyunsaturated fatty acids, lysophospholipids, and Gs, Gi, and Gq protein-coupled receptors. The Journal of biological chemistry 275(37):28398-28405.

McBain CJ, Fisahn A. 2001. Interneurons unbound. Nat Rev Neurosci 2(1):11-23.

McCue HV, Burgoyne RD, Haynes LP. 2009. Membrane targeting of the EF-hand containing calcium-sensing proteins CaBP7 and CaBP8. Biochem Biophys Res Commun 380(4):825-831.

McCue HV, Haynes LP, Burgoyne RD. 2010. The diversity of calcium sensor proteins in the regulation of neuronal function. Cold Spring Harb Perspect Biol 2(8):a004085.

Meuth S, Pape HC, Budde T. 2002. Modulation of Ca2+ currents in rat thalamocortical relay neurons by activity and phosphorylation. Eur J Neurosci 15(10):1603-1614.

Meyer DF, Mabuchi Y, Grabarek Z. 1996. The role of Phe-92 in the Ca(2+)-induced conformational transition in the C-terminal domain of calmodulin. The Journal of biological chemistry 271(19):11284-11290.

Mikhaylova M, Sharma Y, Reissner C, Nagel F, Aravind P, Rajini B, Smalla KH, Gundelfinger ED, Kreutz MR. 2006. Neuronal Ca2+ signaling via caldendrin and calneurons. Biochim Biophys Acta 1763(11):1229-1237.

Nakajima Y. 1974. Fine structure of the synaptic endings on the Mauthner cell of the goldfish. The Journal of comparative neurology 156(4):379-402.

Obermair GJ, Szabo Z, Bourinet E, Flucher BE. 2004. Differential targeting of the L-type Ca2+ channel alpha 1C (CaV1.2) to synaptic and extrasynaptic compartments in hippocampal neurons. Eur J Neurosci 19(8):2109-2122.

Schwaller B, Meyer M, Schiffmann S. 2002. 'New' functions for 'old' proteins: the role of the calcium-binding proteins calbindin D-28k, calretinin and parvalbumin, in cerebellar physiology. Studies with knockout mice. Cerebellum 1(4):241-258.

Seidenbecher CI, Langnaese K, Sanmarti-Vila L, Boeckers TM, Smalla KH, Sabel BA, Garner CC, Gundelfinger ED, Kreutz MR. 1998. Caldendrin, a novel neuronal calcium-binding protein confined to the somato-dendritic compartment. The Journal of biological chemistry 273(33):21324-21331.

Simkin D, Cavanaugh EJ, Kim D. 2008. Control of the single channel conductance of K2P10.1 (TREK-2) by the amino-terminus: role of alternative translation initiation. The Journal of physiology 586(Pt 23):5651-5663.

Smalla KH, Seidenbecher CI, Tischmeyer W, Schicknick H, Wyneken U, Bockers TM, Gundelfinger ED, Kreutz MR. 2003. Kainate-induced epileptic seizures induce a recruitment of caldendrin to the postsynaptic density in rat brain. Brain research Molecular brain research 116(1-2):159-162.

Sotelo C. 2008. Development of "Pinceaux" formations and dendritic translocation of climbing fibers during the acquisition of the balance between glutamatergic and gamma-aminobutyric acidergic inputs in developing Purkinje cells. The Journal of comparative neurology 506(2):240-262.

Stewart AE, Foehring RC. 2001. Effects of spike parameters and neuromodulators on action potential waveform-induced calcium entry into pyramidal neurons. J Neurophysiol 85(4):1412-1423.

Tepper JM, Bolam JP. 2004. Functional diversity and specificity of neostriatal interneurons. Current opinion in neurobiology 14(6):685-692.

Tippens AL, Lee A. 2007. Caldendrin, a neuron-specific modulator of Cav/1.2 (L-type) Ca2+ channels. The Journal of biological chemistry 282(11):8464-8473.

Toth K, Suares G, Lawrence JJ, Philips-Tansey E, McBain CJ. 2000. Differential mechanisms of transmission at three types of mossy fiber synapse. The Journal of neuroscience : the official journal of the Society for Neuroscience 20(22):8279-8289.

Triller A, Korn H. 1980. Glio-axonic junctional like complexes at the Mauthner cell's axon cap of teleosts: a possible morphological basis for field effect inhibitions. Neurosci Lett 18(3):275-281.

Westenbroek RE, Ahlijanian MK, Catterall WA. 1990. Clustering of L-type Ca2+ channels at the base of major dendrites in hippocampal pyramidal neurons. Nature 347(6290):281-284.

Wingard JN, Chan J, Bosanac I, Haeseleer F, Palczewski K, Ikura M, Ames JB. 2005. Structural analysis of Mg2+ and Ca2+ binding to CaBP1, a neuron-specific regulator of calcium channels. The Journal of biological chemistry 280(45):37461-37470.

Yang J, McBride S, Mak DO, Vardi N, Palczewski K, Haeseleer F, Foskett JK. 2002. Identification of a family of calcium sensors as protein ligands of inositol trisphosphate receptor Ca^{2+} release channels. Proc Natl Acad Sci U S A 99(11):7711-7716.

Yang PS, Alseikhan BA, Hiel H, Grant L, Mori MX, Yang W, Fuchs PA, Yue DT. 2006. Switching of Ca2+-dependent inactivation of Ca(v)1.3 channels by calcium binding proteins of auditory hair cells. The Journal of neuroscience : the official journal of the Society for Neuroscience 26(42):10677-10689.

Yap KL, Ames JB, Swindells MB, Ikura M. 1999. Diversity of conformational states and changes within the EF-hand protein superfamily. Proteins 37(3):499-507.

Zhou FM, Lee CR. 2011. Intrinsic and integrative properties of substantia nigra pars reticulata neurons. Neuroscience 198:69-94.

Zhou H, Kim SA, Kirk EA, Tippens AL, Sun H, Haeseleer F, Lee A. 2004. Ca2+-binding protein-1 facilitates and forms a postsynaptic complex with Cav1.2 (L-type) Ca2+ channels. The Journal of neuroscience : the official journal of the Society for Neuroscience 24(19):4698-4708.

Zhou H, Yu K, McCoy KL, Lee A. 2005. Molecular mechanism for divergent regulation of $Ca_v1.2$ Ca^{2+} channels by calmodulin and Ca^{2+}-binding protein-1. J Biol Chem 280(33):29612-29619.